Journal of Applied Research in Water and Wastewater
E-ISSN: 2476-6283
Journal homepage: https://arww.razi.ac.ir

# PVP versus trimesic acid in PES membranes: A direct comparative study of morphology, permeability and antifouling response

**Azar Asadi*, Soheila Hamidi, Samin Sedaghatfard, Hadi Naderi**

*Department of Applied Chemistry, Faculty of Gas and Petroleum, Yasouj University, Gachsaran, Iran.*

## GRAPHICAL ABSTRACT

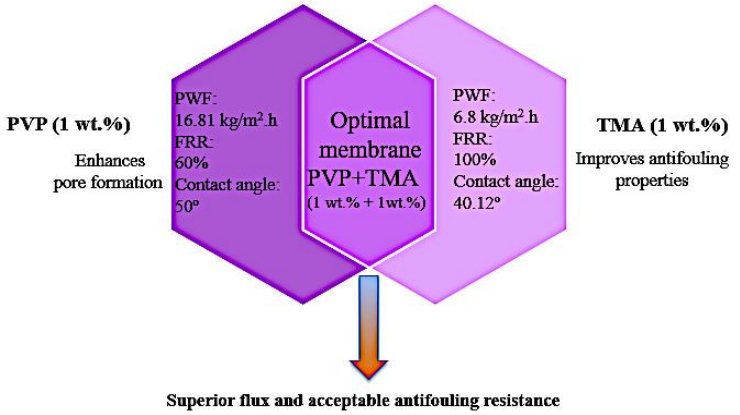


## ARTICLE INFO

**Article type:**
Research Article

**Article history:**
Received xx Month xxx
Reviewed xx Month xxx
Received in revised form xx Month xxx
Accepted xx Month xxx

**Keywords:**
Antifouling
Pure water flux
Synergistic effect
Trimesic acid



## ABSTRACT

This study presents a direct comparative and synergistic investigation of polyvinylpyrrolidone (PVP) and trimesic Acid (TMA) as additives for polyethersulfone (PES) membranes. Scanning electron microscopy (SEM) analysis revealed that PVP primarily acts as a pore-forming agent, while TMA induces a finer, sponge-like morphology. Water contact angle (WCA) measurements confirmed that TMA imparts higher surface hydrophilicity (37.5°) compared to PVP, attributed to its lower aqueous solubility and greater retention of hydrophilic carboxylic acid groups within the polymer matrix. Pure water flux (PWF) data, monitored at 4 bar pressure, showed that membranes embedded with TMA as a single additive had lower flux than the bare membrane, due to their sponge-like pore structure. A powerful synergistic effect was discovered in dual-additive formulations. The optimal membrane (M7), containing 1 wt.% each of PVP and TMA, achieved an exceptional PWF of 103 kg/m²·h. This synergy is driven by accelerated co-leaching during phase inversion, which optimizes pore structure. From the antifouling test, single TMA-based membranes demonstrated the highest FRR values (approximate 100%). Meanwhile, the membranes containing both PVP and TMA showed compromised FRR. Nevertheless, M7 membrane maintained an acceptable FRR of 75%. The results indicate that combining PVP and TMA creates a synergistic effect, producing membranes with a superior balance of high permeability and antifouling resistance compared to those with a single additive.

### 1. Introduction

The global challenge of water scarcity, coupled with the increasing demands of industrial separation processes, has propelled membrane technology to the forefront of scientific and engineering innovation (Goh, Wong and Ismail, 2022; Shannon *et al*., 2008). Among various membrane-based separation techniques, ultrafiltration (UF) occupies a critical niche, effectively separating macromolecules, colloids, and

*Corresponding author Email: a.asadi@yu.ac.ir, azarasadi_88@yahoo.com

Cite this article: A. Asadi, S. Hamidi, S. Sedaghatfard, H. Naderi, PVP versus trimesic acid in PES membranes: A direct comparative study of morphology, permeability and antifouling response, *Journal of Applied Research in Water and Wastewater*, x (x), 202x, xx-xx. doi: https://doi.org 10.22126/arww.2025.13123.1441

suspended solids from solvents based on size exclusion (Shi *et al.*, 2014). The efficacy of an ultrafiltration process is intrinsically tied to the properties of the membrane itself including its porosity, pore size distribution, surface morphology, hydrophilicity, and mechanical strength (Jalali *et al.*, 2023; Kumar and Ismail, 2015). Consequently, the quest to engineer membranes with superior performance that balance high permeability, excellent selectivity, and robust antifouling properties is a central theme in materials science and chemical engineering ( Dolatshah, Ataie, and Asadi, 2022; Werber, Osuji, and Elimelech, 2016).

This pursuit has led researchers to explore a vast array of materials and fabrication techniques. While numerous polymers are employed, polysulfone (PSf) (Serbanescu Serbanescu, Voicu and Thakur, 2020) and its derivative, polyethersulfone (PES), have emerged as main polymers in the UF membrane industry (Asadi *et al.*, 2022b). Their popularity stems from exceptional mechanical strength, thermal stability, and chemical resistance (Otitoju, Ahmad, and Ooi, 2018). However, these hydrophobic polymers have a significant drawback which they are highly prone to fouling (Zhang *et al.*, 2016). Organic molecules, proteins, and other contaminants readily adsorb onto their surfaces which leads to clogging pores, drastically reducing flux, and increasing operational costs through frequent cleaning and reduced membrane lifespan (Rana and Matsuura, 2010). To overcome this limitation, the field has turned to the art of membrane modification (Asadi *et al.*, 2022a). A particularly powerful and prevalent method is the blending modification technique, where additives are introduced into the polymer dope solution before the phase inversion process. Among these additives, PVP has long been a staple pore-forming agent and hydrophilic modifier (Kourde-Hanafi *et al.*, 2017). Although PVP leaches out during coagulation, studies using techniques like Fourier-Transform Infrared (FTIR) and X-ray photoelectron spectroscopy (XPS) have confirmed that a fraction of PVP molecules remains entrapped within the polymer matrix of the membrane (Yuliwati and Esmail, 2011). These residual PVP molecules are a boon for performance. PVP is rich in polar carbonyl (C=O) groups in its pyrrolidone ring. These groups migrate to the membrane-water interface during phase inversion, reducing the surface energy and significantly increasing the membrane's hydrophilicity (Eren and Güney, 2019). A hydrophilic surface attracts water molecules, forming a protective hydration layer that acts as a barrier against hydrophobic foulants like proteins and organic oils. This directly translates to improved antifouling properties and enhanced flux recovery (Mavukkandy *et al.*, 2016).

More recently, the exploration of organic acids such as trimesic acid (TMA), has revealed new avenues for creating advanced membrane structures. Unlike polymeric PVP, small molecule TMA can be more uniformly distributed in the dope and can lead to the formation of smaller, more numerous nuclei during phase separation (Gu *et al.*, 2021). This often results in a membrane with a narrower pore size distribution and smaller average pore sizes compared to a PVP-modified membrane (Qu *et al.*, 2020). This enhances the membrane's selectivity and the polar carboxylic acid groups of TMA can also impart hydrophilicity to the membrane surface(Kumar *et al.*, 2019).

This research delves into the individual and, more importantly, the synergistic effects of PVP and TMA on the fabrication, morphology, and performance of PES membranes, illustrating how their combination represents a sophisticated tool for tailoring membrane properties. The literature frequently documents TMA for its dual applications as a polymer co-monomer and a building block for MOFs (Asadi et al., 2025) In contrast, this work systematically evaluates TMA's role by examining its impact both individually and in combination with PVP, thereby isolating its specific contribution to membrane performance. Also, this study employed two significantly different PVP concentrations (1 wt.% and 10 wt. %) in the bare membrane formulation to explicitly highlight its role in governing pure water flux, hydrophilicity, and antifouling properties.

## 2. Materials and methods

### 2.1. Materials

Polyethersulfone (PES, MW = 58,000 g/mol) was chosen as the main polymer, and dimethylacetamide (DMAc) was used as the solvent. PES and DMAc were purchased from BASF and Merck, respectively.

### 2.2. Preparation of membranes

Membranes were fabricated using the casting solution compositions specified in Table 1. To ensure homogeneity, the mixtures were stirred continuously for 24 h and subsequently sonicated for 30 min in degas mode (Bandelin DT 102H ultrasonic device, Germany). The resulting uniform solutions were cast onto glass plates at a thickness of 150 µm using a casting knife. The plates were then immediately immersed in a non-solvent bath of distilled water to initiate phase inversion. The formed polymeric membranes were subsequently transferred to fresh distilled water for 24 h to complete the phase separation process. Then, the newly cast membranes were then left to dry at room temperature while pressed between filter papers (Gholami *et al.*, 2018; Zinadini *et al.*, 2014).

**Table 1.** Casting solution composition of the prepared membranes.

| Membrane type | PES, (wt.%) | PVP, (wt.%) | TMA, (wt.%) | DMA, (wt.%) |
|---|---|---|---|---|
| $M_1$ | 18.0 | 1.0 | 0 | 81.0 |
| $M_2$ | 18.0 | 10.0 | 0 | 72.0 |
| $M_3$ | 18.0 | 0 | 0.5 | 81.5 |
| $M_4$ | 18.0 | 0 | 1.0 | 81.0 |
| $M_5$ | 18.0 | 0 | 2.0 | 80.0 |
| $M_6$ | 18.0 | 1.0 | 0.5 | 80.5 |
| $M_7$ | 18.0 | 1.0 | 1.0 | 80.0 |
| $M_8$ | 18.0 | 1.0 | 2.0 | 79.0 |

### 2.3. Characterizations of the fabricated membranes

To characterize the prepared membrane, its morphology was examined by Scanning Electron Microscopy (SEM) (Philips XL30, Netherlands), surface wettability was assessed through water-contact-angle measurements (XCA-50 goniometer), and chemical functionality was analyzed with Attenuated Total Reflectance Fourier-Transform Infrared (ATR-FTIR, Bruker Alpha, Germany).

### 2.4. Performance tests

Membrane performance was assessed in a stainless-steel, dead-end cell (150 mL capacity, 12.54 cm² active area). Nitrogen was used to supply a trans-membrane pressure of 4 bar. After applying this pressure for 15 minutes, the permeate mass was logged with a digital balance and used in Eq. 1 to compute the pure water flux**.**

$$J_{w.1} = \frac{M}{A\Delta t} \quad (1)$$

here, $J_{w.1}$ denotes the pure water flux (kg/m².h), M is the mass of permeate collected (kg), the effective membrane area (m²), and Δt is the sampling interval (h). Antifouling behavior was probed with 1000 ppm milk powder as a model protein foulant. The following sequential steps were performed: (1) passing distilled water through each membrane for 60 min; (2) filtering the milk powder solution for 90 min; (3) cleansing each membrane with distilled water for 10 min; and (4) determining the second pure water flux for a further 60 min. Between cycles the cell was flushed for 10 min with fresh water. The flux recovery ratio (FRR) was then calculated from the corresponding permeate data using Eq. 2.

$$FRR = \left(\frac{Jw2}{Jw1}\right) \times 100 \quad (2)$$

In which $J_{w,1}$ and $J_{w,2}$ are the PWFs measured before and after the milk powder challenge, respectively.

## 3. Results and discussion

### 3.1. Membrane characteristics

Cross-sectional SEM images of the fabricated membranes are displayed in Fig. 1. Comparative analysis of M1 and M2 (Fig. 1 a and b), which vary solely in PVP dosage, indicates that an increase in PVP from 1 to 10 wt.% improved pore density and resulted in a narrower pore size distribution, affirming its function as a pore-forming agent. Also, the effects of TMA as an alternative additive were examined in membranes M3, M4, and M5. Fig. 1c shows that M3 (0.5 wt.% TMA) exhibited a sponge-like structure with dense surface layer and narrow pores in the sublayer. When the dosage was raised to 1 wt.% (M4), the pore density increased, although the pores remained constricted (Fig. 1d). At 2 wt.% (M5), a real sponge-like structure with thicker top layer could be seen as a result of higher density of casting solution (Fig.1e) (Mi *et al.*, 2001).

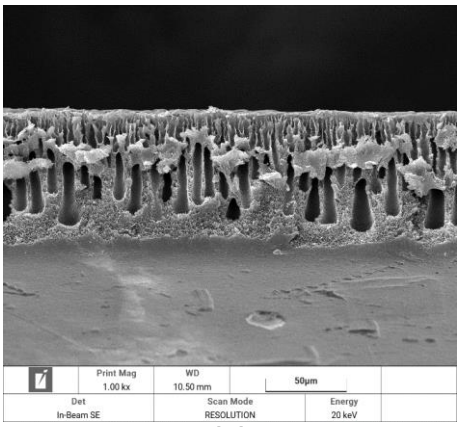


**($a_1$)**

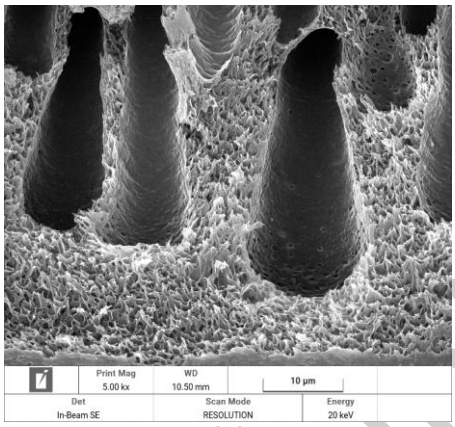


**($a_2$)**

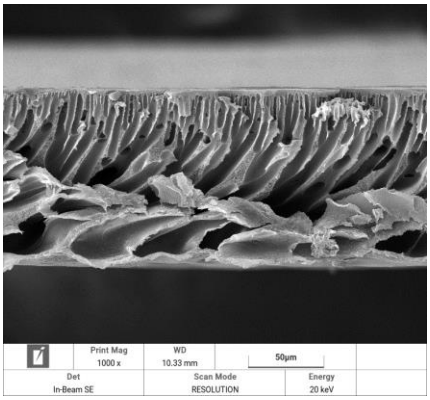


**($b_1$)**

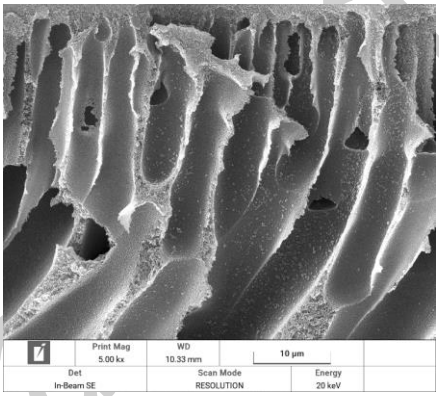


**($b_2$)**

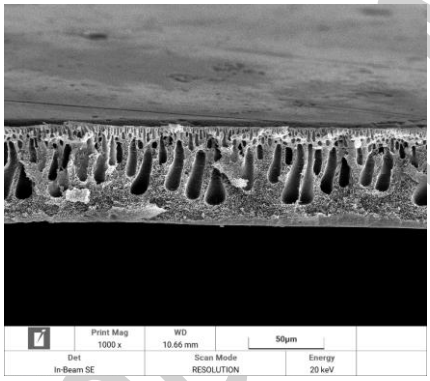


**($c_1$)**

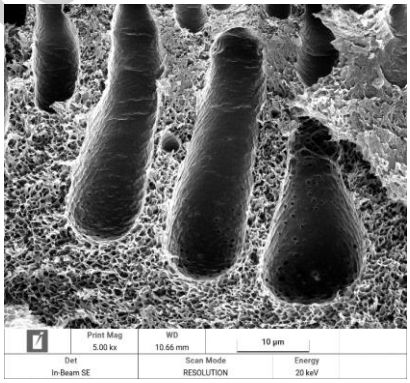


**($c_2$)**

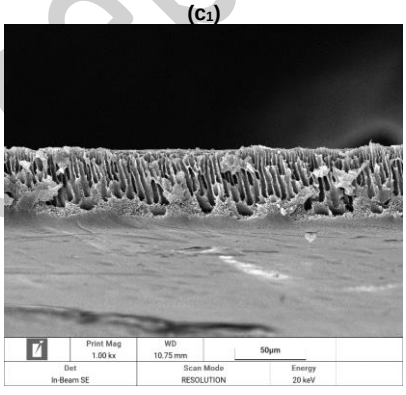


**($d_1$)**

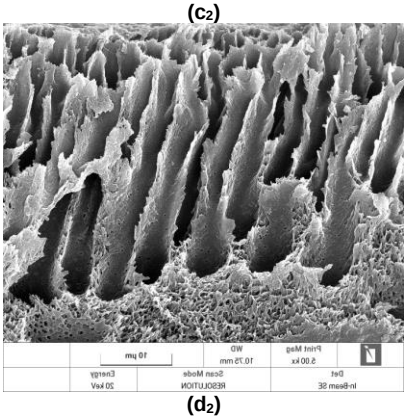

**($d_2$)**

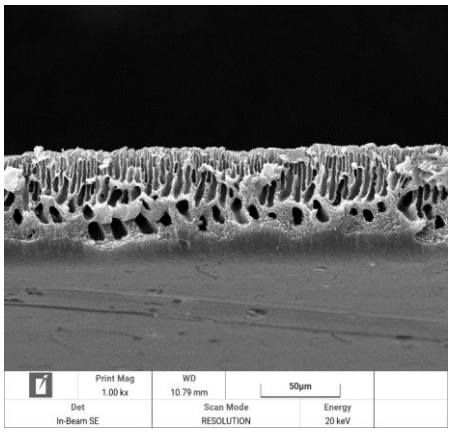


**($e_1$)**

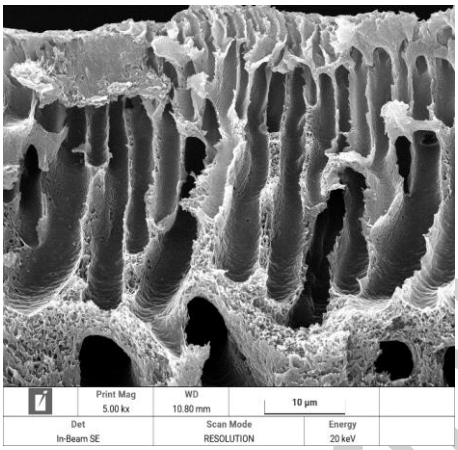


**($e_2$)**

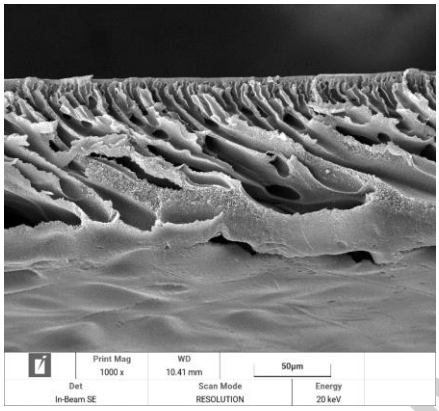


**($f_1$)**

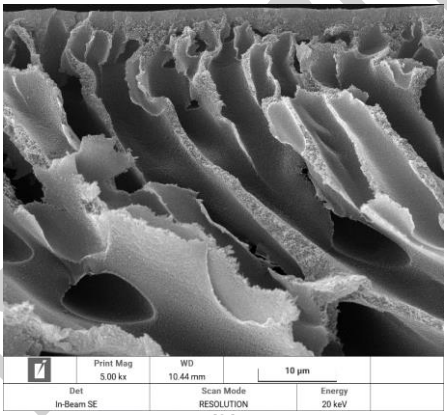


**($f_2$)**

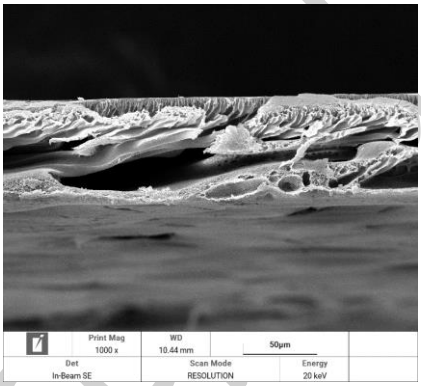


**($g_1$)**

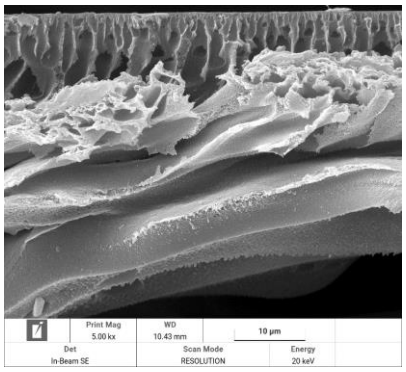


**($g_2$)**

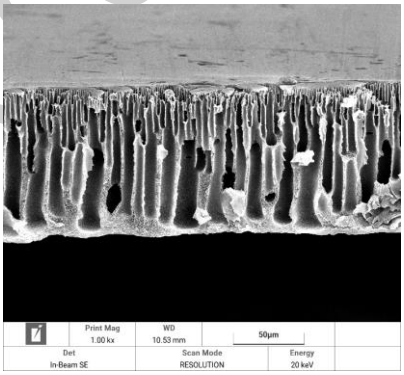


**($h_1$)**

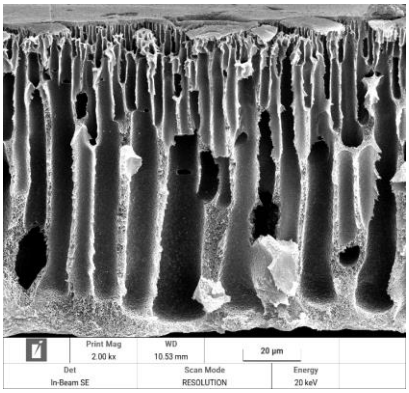


**($h_2$)**

**Fig. 1.** Cross-section SEM images of M1 ($a_{1,2}$): M2 ($b_{1,2}$): M3 ($c_{1,2}$): M4 ($d_{1,2}$): M5 ($e_{1,2}$): M6 ($f_{1,2}$): M7 ($g_{1,2}$): M8 ($h_{1,2}$).

Therefore, based on the reported SEM images, PVP performs better than TMA in forming pore size and pore density. Besides, membranes M6, M7, and M8, which were modified with PVP and TMA (Fig. 1 f, g, and h), developed high density pores that were larger than those in other samples. Increasing TMA from 0.5 to 1 wt.% loosened the surface layer and widened the underlying channels. However, a further increase in concentration to 2 wt.% tightened the surface layer and restricted the channels. This is attributed to the higher density of the casting solution, which delayed phase inversion by impeding the out-diffusion of solvent and the in-diffusion of non-solvent (Tavajohi and Khayet, 2024).

Also, ATR-FTIR spectroscopy was utilized to investigate the chemical functional groups present on the surface of the prepared membranes. Fig. 2a presents the ATR-FTIR spectra for membranes M1 and M2, which were fabricated with different PVP loadings. The spectra confirm the presence of the PES polymer through its key vibrational modes: strong sulfone group peaks at 1320 $cm^{-1}$ (asymmetric) and 1150 $cm^{-1}$ (symmetric), aromatic C=C stretching bands at 1575 and 1480 $cm^{-1}$, and a C-H out-of-plane bending peak at 780 $cm^{-1}$. The presence of PVP is confirmed by its characteristic sharp carbonyl (C=O) stretch at ~1665 $cm^{-1}$, along with a broad O-H stretching band around 3300 $cm^{-1}$ from absorbed water (Athira, Mohanty, and Nayak, 2020). Both of these peaks are significantly more intense in the M1 spectrum. Overall, while the two spectra exhibit identical peak positions, the intensities of all characteristic bands are stronger for M1, which indicates that PVP leached out more completely in M2 with a higher PVP loading (10 wt.%) compared to M1 (1 wt.%).

The ATR-FTIR spectra of membranes M3 to M5, fabricated with different loadings of TMA and without PVP, are displayed in Fig. 2b. A weak peak at approximately 1660 $cm^{-1}$, corresponding to the C=O stretch of TMA, is observed in all three spectra. The intensity of this peak increases consistently with higher TMA loadings from M3 to M5. Furthermore, the O-H stretching band of the carboxylic acid group in TMA is also present and is most noticeable in membrane M5, which contained the highest TMA dosage (Hayat *et al*., 2019). Other characteristic peaks of trimesic acid arising from its benzene ring overlap with the peaks of PES. Finally, Fig. 2c presents the ATR-FTIR spectra of membranes M6 to M8. These membranes are equivalent to M3-M5 in TMA content, but were fabricated with the addition of PVP (1 wt.%). The peaks for the C=O stretch (~1660 $cm^{-1}$) are more intense and distinct in these spectra, as both the TMA and PVP components contribute carbonyl groups.

### 3.2 Hydrophilicity and PWF

To investigate hydrophilicity of the fabricated membranes, contact angles of each membrane have been reported in Fig. 3a. Comparing the results obtained for M1 and M2, it was found that higher percentages of PVP decrease the surface hydrophilicity of the fabricated membrane, as the contact angle increased from 50° for M1 (with 1 wt.% PVP) to 60.75° for M2 (with 10 wt.% PVP), attributed to complete leaching that left large voids, as shown in Fig. 1b. As a fact, PVP leaches out more rapidly during coagulation due to its higher concentration; this outcome is confirmed by the FTIR results discussed earlier (see Fig. 2a). Although PVP's leaching is kinetically limited by its high molecular weight and chain entanglement, an increased dosage enhances its own mobility and concentration gradient, thereby promoting more complete removal during phase inversion (Xu and Qusay, 2004).

Besides, the contact angles of M3, M4, and M5 represent the effect of TMA on the hydrophilicity of the fabricated membranes. As observed, the contact angles for 0.5 to 2 wt.% TMA were in the range of 43.95° to 37.56°, indicating a higher potential of TMA to increase membrane surface hydrophilicity compared to PVP. This result can be attributed to the lower solubility of TMA in water compared to PVP (Moschidou *et al*., 2013).

In M6, M7, and M8, the synergistic effect of PVP and TMA has been investigated with 1 wt.% PVP and 0.5, 1, and 2 wt.% TMA, respectively. As a result, the contact angles of M6, M7, and M8 were higher than their equivalents in terms of TMA content but without PVP (M3, M4, and M5). This results proves that the presence of PVP accelerate leaching out TMA from polymer matrix during phase inversion leading to an increase in contact angles in the range of 46.84º to 49.41º.

Also, PWF is a key performance metric for membranes, therefore the PWF of the fabricated membranes is presented in Fig. 3b. The PWF increased from 16.81 kg/m²·h for M1 to 31.59 kg/m²·h for M2, corresponding to an increase in PVP concentration from 1 to 10 wt.%. This significant rise is a direct result of PVP's pore-forming nature. This finding aligns with the SEM images in Fig. 1a and b, where M2 exhibits a visibly greater pore density.

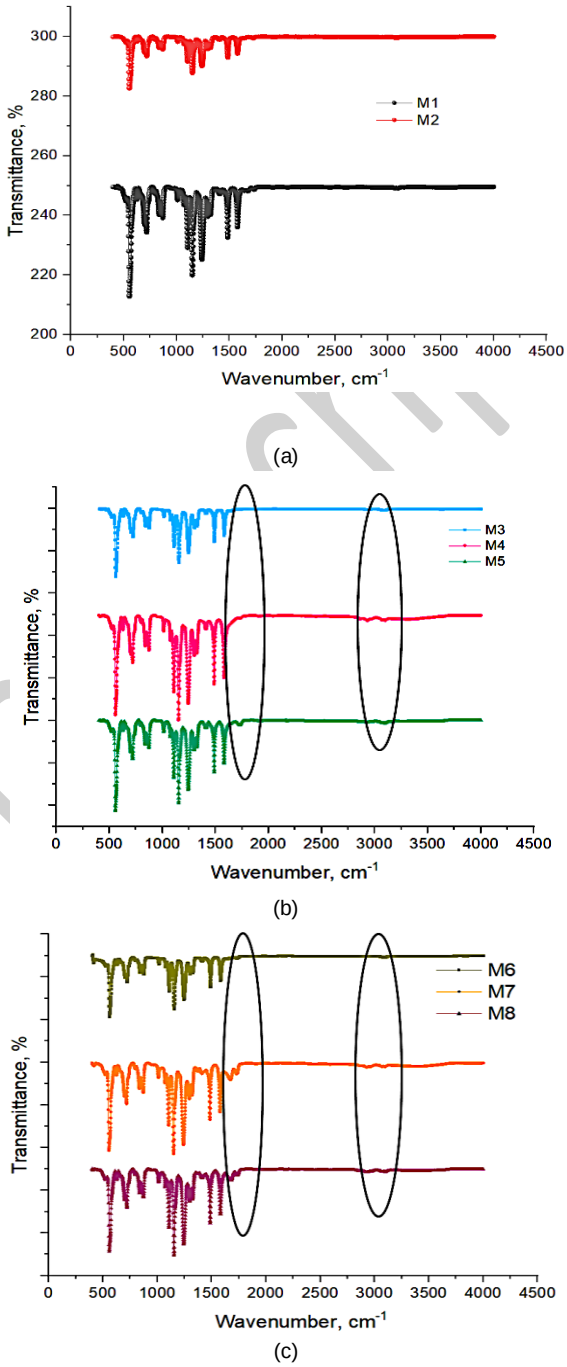


**Fig.2**. ATR-FTIR spectrum of M1 and M2 (a); M3, M4, and M5 (b); M6, M7, and M8 (c).

Membranes M3, M4, and M5, which contained varying loadings of TMA but no PVP, exhibited very low PWF. The PWF for M3 (0.5 wt.% acid) was negligible, while M4 (1 wt.% acid) reached only 6.8 kg/m²·h. A direct comparison between M1 and M4, which share the same concentrations of PVP and TMA, respectively, confirms the high efficacy of PVP in pore formation compared to TMA (16.81 versus 6.8 kg/$m^2$.h for M1 and M4, respectively).

The incorporation of both 1 wt.% PVP and 0.5 wt.% TMA (M6) resulted in a PWF of 54 kg/m²·h. This synergistic effect, which enhanced PWF, is verified by the enlarged channels observed in SEM images. The PWF increased further with higher TMA loading, peaking at 103 kg/m²·h for membrane M7. The synergistic interaction between TMA and PVP

enhances the leaching kinetics of both compounds during the phase inversion process, leading to the optimized structure responsible for the maximum performance. This optimal performance at a specific ratio of PVP to TMA demonstrates a successfully engineered synergy, similar to that reported for other polymer-organic acid systems, leading to a membrane with significant permeability (Mulyati *et al*., 2025).

However, increasing the TMA concentration to 2 wt.% (M8) significantly reduced the pure water flux (PWF) to 22.79 kg/m²·h. This decline is attributed to the higher density of the casting solution, which delayed the phase inversion process and resulted in a tighter pore structure, as shown in Fig. 1h. In conclusion, the synergistic combination of 1 wt.% PVP and 1 wt.% TMA in the casting solution produced a superior enhancement in pure water flux (PWF). This optimal formulation renders higher PVP loadings unnecessary, as a 10 wt.% PVP additive alone increased PWF by only two-fold, while the inclusion of 1 wt.% TMA boosted it by six-fold.

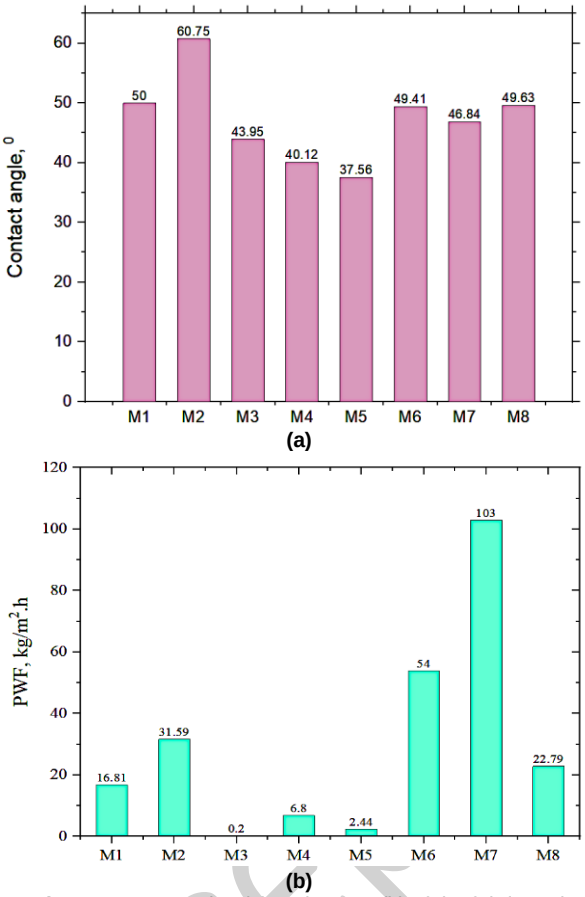


**Fig.3.** Contact angles (a) and PWFs (b) of the fabricated membranes.

### 3.3. Antifouling properties

The antifouling performances of the fabricated membranes were evaluated using a three-step filtration protocol (distilled water, milk powder solution, distilled water), with the data presented in Fig. 4 a, b, and c. Besides, in order to further evaluate antifouling property of the fabricate membranes, flux recovery ratio (FRR) index has been calculated based on the obtained data and displayed in Fig. 4d. As shown in Fig. 4a, both M1 and M2 (with 10 wt.% PVP) exhibits low antifouling resistance, demonstrating a significant decline in performance during milk powder filtration, however flux of M2 was higher at all three steps. Moreover, FRR values was declined by increasing PVP dosage from 1 to 10 wt.% so that FRR were 60 and 54% for M1 and M2, respectively. These findings suggest that at higher concentrations, PVP can be substantially leached out, functioning primarily as a sacrificial pore-former as discussed earlier. Consequently, the decrease in surface hydrophilic groups on membrane M2 resulted in a higher water contact angle (see Fig. 3a). therefore, this loss of hydrophilicity directly reduced the membrane's antifouling performance.

The antifouling performance of membranes M4 and M5, which were embedded with TMA, is presented in Fig. 4b. It should be mentioned that the data for M3 is absent because its negligible PWF precluded a meaningful FRR measurement. From the results, M4 (0.5 wt.% TMA) and M5 (1 wt.% TMA) demonstrated a significant ability to recover their PWF after milk powder filtration. On the other hand, 100% and 95% of FRR values were reported for M4 and M5, respectively. The performance correlates with the hydrophilic character indicated by Fig. 3a. The low PWF of M4 and M5 reveals that TMA is retained in the matrix more than PVP and is a less effective porogen. Nonetheless, this embedded TMA enhances surface cleanability, leading to the observed combination of low initial flux and high flux recovery.

Furthermore, a three-step filtration test was performed for membranes M6, M7, and M8, which were embedded with both PVP and TMA and the results are presented in Fig. 4c. The data indicate that these membranes showed lower resistance to milk powder filtration compared to the membrane embedded with TMA lonely. This outcome could be related to the superior PWF which previously explained. As a fact, enhancing PWF sacrifices antifouling resistance as a result of higher enlarger pores resulting from accelerating leaching TMA and PVP. Based on these results, the antifouling performance can be ranked as M7 > M6 > M8. The FRR data further validated this order, with M7 exhibiting FRR at 75%, followed by M6 at 52%, and finally M8 at 32%. This trend shows that with a constant 1 wt.% PVP, increasing TMA loading from 0.5 wt.% to 1 wt.% improved antifouling persistence, however, a further increase to 2 wt.% had a detrimental effect. This reversal can be explained by the membrane's morphology which based on the SEM images in Fig. 1, at higher TMA loading (2 wt.%) limited pore size and channels were observed. This constricted morphology ultimately resulted in a lower pure water flux and diminished antifouling performance.

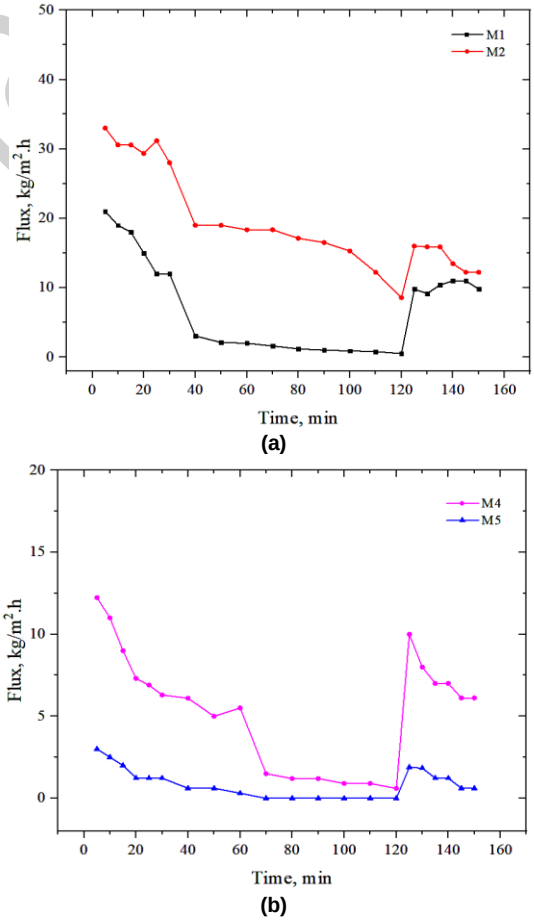

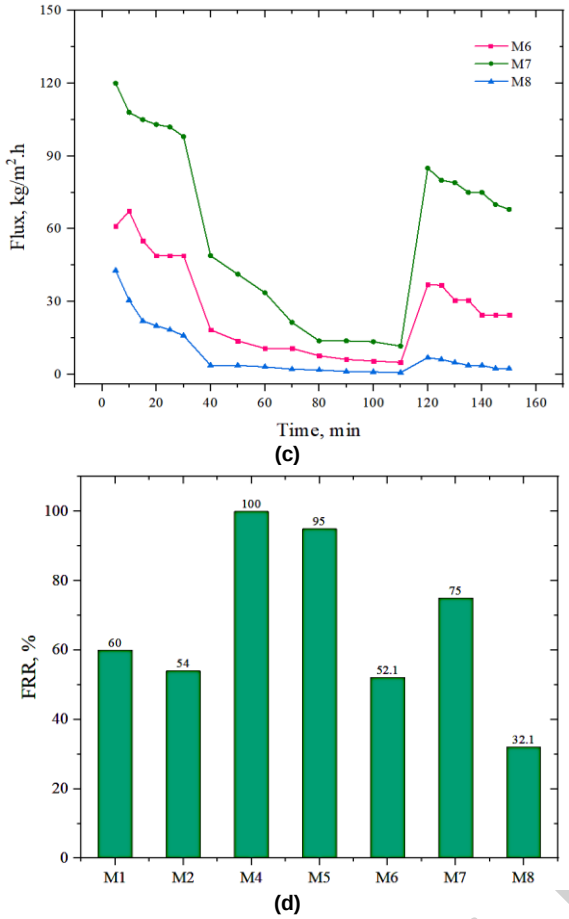


**Fig. 4.** Three-step filtration performance of M1 and M2 (a); M3, M4, and M5 (b); M6, M7, and M8 (c); and FRR of the fabricated membranes (d).

## 4. Conclusions

This study demonstrates that combining the polymeric pore-former PVP with the small-molecule hydrophilicity agent TMA creates a powerful synergy for engineering PES membranes. Individually, PVP boosts permeability but offers limited antifouling gain, while TMA enhances surface cleanability but severely restricts flux. However, a strategic combination of both TMA and PVP (1 wt.% each) overcomes the trade-off between permeability and antifouling properties. The optimal membrane (M7) achieves an exceptional six-fold increase in pure water flux (103 kg/m²·h) while maintaining an acceptable flux recovery ratio of 75 %. This synergy allows for precise tailoring of membrane morphology and surface properties, ultimately resulting in a membrane with an ideal balance of high permeability and a satisfactory antifouling performance, surpassing the capabilities of single-additive formulations.

## Author Contributions

Azar Asadi: Conceived and designed, reviewing and editing the manuscript
Soheila Hamidi, Hadi Naderi, and Samin Sedaghatfard: Performed the experiments, collected and analyzed the data, and wrote the first draft of the manuscript.

## Conflict of Interest

The authors declare that they have no competing interests.

## Acknowledgment

The authors acknowledge Yasouj University, Yasouj, Iran, for its full financial support.

## Data Availability Statement

All data generated or analyzed during this study are included in this published article.

## References

Asadi, A. *et al.* (2025) 'Enhancing filtration performance and recovery potential of polyvinylidene fluoride membrane by incorporating MOF@MWCNT: Using synthetic and real foulants', *Journal of Water Process Engineering*, *69*, p. 106731. doi: https://doi.org/10.1016/j.jwpe.2024.106731

Asadi, A. *et al.* (2022a) 'Improved filtration performance of polyvinylidene fluoride nanocomposite membranes embedded with deep eutectic solvent: Application towards MBR', *Desalination, 543*, p. 116088. doi: https://doi.org/10.1016/j.desal.2022.116088

Asadi, A. *et al.* (2022b) 'Application of novel nanofiltration membranes embedded with mesoporous carbon based nanoparticles for desalination and dye removal', Chemical Papers, *76(3)*, pp. 1349-1363. doi: https://doi.org/10.1007/s11696-021-01944-w

Athira, V. B., Mohanty, S. and Nayak, S. K. (2020) 'Preparation and characterization of porous polyethersulfone (PES) membranes with improved biocompatibility by blending sulfonated polyethersulfone (SPES) and cellulose acetate phthalate (CAP)', *Materials Today Communications*, *25*, p. 101629. doi: https://doi.org/10.1016/j.mtcomm.2020.101544

Dolatshah, M., Ataie, M., and Asadi, A. (2022.) 'A Review on the performance of modified polymeric ultrafiltration membranes to reduce fouling phenomena for wastewater treatment', *Journal of Water and Wastewater Science and Engineering*, *7(4)*, pp. 17-29. doi: https://doi.org/10.22112/jwwse.2022.336156.1314

Eren, B., and Güney, M. (2019) 'The role of polyvinylpyrrolidone as a pore former on microstructure and performance of polysulfone membranes', *Bilecik Sheikh Edebali University Journal of Science*, *6*, pp. 168-176. doi: https://doi.org/10.35193/bseufbd.589808

Gholami, F. *et al.* (2018) 'TMU-5 metal-organic frameworks (MOFs) as a novel nanofiller for flux increment and fouling mitigation in PES ultrafiltration membrane', Separation and Purification Technology, *194*, pp. 272-280. doi: https://doi.org/10.1016/j.seppur.2017.11.054

Goh, P., Wong, K. and Ismail, A. (2022). 'Membrane technology: A versatile tool for saline wastewater treatment and resource recovery', Desalination, 521, p. 115377. doi: https://doi.org/10.1016/j.desal.2021.115377

Gu, K. *et al.* (2021) 'Ion-promoting-penetration phenomenon in the polyethyleneimine/trimesic acid nanofiltration membrane', *Separation and Purification Technology*, 257, p. 117958. doi: https://doi.org/10.1016/j.seppur.2020.117958

Hayat, A. *et al.* (2019) 'Synthesis and optimization of the trimesic acid modified polymeric carbon nitride for enhanced photocatalytic reduction of $CO_2$', *Journal of Colloid and Interface Science*, 548, pp. 197-205. doi: https://doi.org/10.1016/j.jcis.2019.04.037

Jalali, F. *et al.* (2023) 'A moving bed biofilm reactor coupled with an upgraded nanocomposite polyvinylidene fluoride membrane to treat an industrial estate wastewater', *Chemical Engineering Journal*, 470, p. 144128. doi: https://doi.org/10.1016/j.cej.2023.144128

Kourde-Hanafi, Y. *et al.* (2017) 'Influence of PVP content on degradation of PES/PVP membranes: Insights from characterization of membranes with controlled composition', *Journal of Membrane Science*, 533, pp. 261-269. doi: https://doi.org/10.1016/j.memsci.2017.01.041

Kumar, R. *et al.* (2019) 'Boron selective thin film composite nanofiltration membrane fabricated via a self-assembled trimesic acid layer at a liquid–liquid interface on an ultrafiltration support', *New Journal of Chemistry*, *43(9)*, pp. 3874-3883. doi: https://doi.org/10.1039/C8NJ05691A

Kumar, R., and Ismail, A. (2015) 'Fouling control on microfiltration/ultrafiltration membranes: Effects of morphology,

hydrophilicity, and charge', *Journal of Applied Polymer Science*, *132(21)*, p. 41942. doi: https://doi.org/10.1002/app.42042

Mavukkandy, M.O. *et al*. (2016)' Leaching of PVP from PVDF/PVP blend membranes: impacts on membrane structure and fouling in membrane bioreactors', Journal of Materials Science, *51(9),* pp. 4328-4341. doi: https://doi.org/10.1007/s10853-016-9748-3

Mi, F.L. et al. (2001) 'Fabrication and characterization of a sponge-like asymmetric chitosan membrane as a wound dressing', *Biomaterials*, 22(2), pp. 165-173. doi: https://doi.org/10.1016/S0142-9612(00)00167-8

Moschidou, D. *et al.* (2013) 'Human mid-trimester amniotic fluid stem cells cultured under embryonic stem cell conditions with valproic acid acquire pluripotent characteristics', *Stem Cells and Development*, 22(3), pp. 444-458. doi: 444-458. https://doi.org/10.1089/scd.2012.0327

Mulyati, S. *et al.* (2025) 'Tailoring PVDF membrane antifouling properties via tannic acid blending and chitosan surface coating', *Results in Chemistry*, *14*, p: 102709. doi: https://doi.org/10.1016/j.rechem.2024.102709

Otitoju, T.A., Ahmad, A.L. and Ooi, B.S. (2018) 'Recent advances in the hydrophilic modification of polyethersulfone (PES) membranes via blending method', *RSC Advances*, 8(40), pp. 22710-22734. doi: https://doi.org/10.1039/C8RA03296C

Qu, S. *et al.* (2020) 'Improving the proton conductivity of sulfonated poly (ether ether ketone) membranes by incorporating a crystalline nanoassembly of trimesic acid and melamine', *International Journal of Hydrogen Energy*, 45(54), p. 29883-29891. doi: https://doi.org/10.1016/j.ijhydene.2019.09.226

Rana, D., and Matsuura, T. (2010) 'Surface modifications for antifouling membranes'. *Chemical Reviews*, 110(4), pp. 2448-2471. doi: https://doi.org/10.1021/cr800208y

Serbanescu, O., Voicu, S. and Thakur, V. (2020) 'Polysulfone functionalized membranes: Properties and challenges', Materials Today Chemistry, *17*, p. 100302. doi: https://doi.org/10.1016/j.mtchem.2020.100302

Shannon, M.A. *et al.* (2008) 'Science and technology for water purification in the coming decades', Nature, 452(7185), pp. 301-310. doi: https://doi.org/10.1038/nature06599

Shi, X. *et al.* (2014) 'Fouling and cleaning of ultrafiltration membranes: A review', Journal of Water Process Engineering, *1*, pp. 121-138. doi: https://doi.org/10.1016/j.jwpe.2014.04.003

Tavajohi, N., and Khayet, M. (2024) *Polymeric Membrane Formation by Phase Inversion*. 1st edn. Oxford: Elsevier.

Werber, J.R., Osuji, C.O., and Elimelech, M. (2016) 'Materials for next-generation desalination and water purification membranes'. Nature Review Materials, *1(5)*, pp: 1-15. doi: https://doi.org/10.1038/natrevmats.2016.18

Xu, Z.L., and Qusay, F.A. (2004) 'Polyethersulfone (PES) hollow fiber ultrafiltration membranes prepared by PES/non-solvent/NMP solution', Journal of Membrane Science, *233(1-2)*, pp. 101-111. doi: https://doi.org/10.1016/j.memsci.2004.01.009

Yuliwati, E., and Ismail, A.F (2011) 'Effect of modified PVDF hollow fiber submerged ultrafiltration membrane for refinery wastewater treatment', *Desalination*, *283*, pp. 214–220. doi: https://doi.org/10.1016/j.desal.2011.03.049

Zhang, R., *et al.* (2016) 'Antifouling membranes for sustainable water purification: strategies and mechanisms', Chemical Society Reviews, *45(21)*, pp. 5888-5924. doi: https://doi.org/10.1039/C5CS00579E

Zinadini, S. *et al.* (2014) 'Preparation of a novel antifouling mixed matrix PES membrane by embedding graphene oxide nanoplates', Journal of Membrane Science, *453*, pp. 292-301. doi: https://doi.org/10.1016/j.memsci.2013.10.070